Int J Thermophys (2007) 28:1775–1788
DOI 10.1007/s10765-007-0266-z

Progress Towards an Acoustic Measurement of the Molar Gas Constant at INRIM

R. M. Gavioso · G. Benedetto · P. A. Giuliano Albo · A. Merlone · A. Balsamo · G. E. D'Errico · R. Spagnolo

Published online: 11 October 2007

Abstract Progress in developing an experiment for the determination of the molar gas constant R and the Boltzmann constant k at INRIM is reported. The experiment involves simultaneous measurements of the acoustic and microwave resonance frequencies of a stainless steel spherical resonator for which its hemispheres were deliberately misaligned. For the present work, these frequencies were measured in helium near 273.16 K, in the pressure range from 100 to 800 kPa. From microwave data, the radius of the resonator was determined as a function of pressure with an estimated uncertainty of 6.0 ppm. Using acoustic data and the microwave determination of the resonator radius, the speed of sound in helium was deduced, and these values were compared with those predicted by recent accurate *ab initio* calculations. Over most of the pressure range, the present values agreed with the *ab initio* values within the uncertainty of the measurements (standard uncertainty of approximately 7.0 ppm). Many suggestions for reducing the uncertainty are provided.

Keywords Boltzmann constant · Molar gas constant · Primary acoustic thermometry · Speed of sound

1 Introduction

The INRIM research project to determine the molar gas constant R and the Boltzmann constant k is pursued within the framework of an international collaboration agreement, involving several other European Metrological Institutes and Universities (PTB,

R. M. Gavioso (✉) · G. Benedetto · P. A. Giuliano Albo · A. Merlone · R. Spagnolo
Thermodynamics Division, Istituto Nazionale di Ricerca Metrologica, Torino, Italy
e-mail: gavioso@inrim.it

A. Balsamo · G. E. D'Errico
Mechanics Division, Istituto Nazionale di Ricerca Metrologica, Torino, Italy

NPL, LNE-INM/CNAM, Universitè Paris Nord, University of Naples, Polytechnic of Milan). The goal is the determination of k with an uncertainty of 1 ppm or less using several different experimental methods. If achieved within the next few years, this joint research effort will support the adoption of a new definition of the kelvin, based on the assignment of an exact fixed value to k.

Recently, significant advances in the experimental practice and theory of quasi-spherical resonators have demonstrated the usefulness and the accuracy achievable in their application to acoustic primary thermometry [1–5] and the development of a helium-based pressure standard [6]. These instruments rely on a measurement of resonance frequency ratios, either as a function of temperature or a function of pressure, which are usually determined with extremely high precision and accuracy, despite the perturbation induced by the imperfect geometrical shape of the resonator. In principle, an acoustic determination of R or k needs an *absolute* dimensional characterization of the resonator at 273.16 K. However, if microwave measurements are used for this purpose, the task is equivalent to verifying that the same cavity radius (or volume) is sensed by the acoustic waves and the electromagnetic field as a function of pressure.

In this work, we determined the *microwave* radius of a deliberately misaligned stainless steel resonator by measuring the resonance frequencies of five triply degenerate microwave modes, when the resonator was filled with helium between 100 and 800 kPa at a temperature close to 273.16 K. Over the whole pressure range, we compared our experimental values of speed of sound in helium, v_{exp}, with the theoretical values, v_{theory}, predicted using recent, accurate *ab initio* calculations of the helium–helium potential [7]. We found that v_{exp} and v_{theory} agree within their combined uncertainty of approximately 7.8 ppm. (Unless stated otherwise, all uncertainties are one standard uncertainty.)

At present, the accuracy of our determination of v_{exp} is mainly limited by a few sources of uncertainty: (i) our imperfect modeling of certain acoustic perturbations, including the admittance of the shell and that of a vent-hole, both of which cause a dispersion among the results obtained from different modes; (ii) a discrepancy between the experimental half-widths of microwave modes and the value of the same quantities as calculated from literature values of the electrical resistivity of stainless steel. This discrepancy, which currently amounts to 6.0 ppm, is reduced to 2.5 ppm, if the electrical resistivity of steel is fitted to the experimental data, or equivalently if experimental half-widths are used to correct the frequency perturbation arising from the skin effect (*i.e.*, the penetration of the microwave fields into the steel); and (iii) our current incomplete knowledge regarding the internal geometry of the assembled resonator and the lack of a suitable mathematical model that accounts for the perturbation of the average frequency of the microwave modes by this imperfect geometry.

We denote the relative uncertainty in the calculation of v_{theory} by $u_r(v_{\mathrm{theory}})$. At zero pressure, $u_r(v_{\mathrm{theory}}) = u_r(R)/2$, where $u_{\mathrm{r}}(R) = 1.8$ ppm is the relative uncertainty of the accepted value of the molar gas constant. At 800 kPa, the highest experimental pressure investigated in this work, $u(v_{\mathrm{theory}})$ is dominated by the uncertainty of the *ab initio* value of the second virial coefficient B. Within these limits, accurate measurements of the speed of sound in helium may validate the equivalence of the *microwave* and the *acoustic* resonator radius; alternatively, they may be used for an

acoustic calibration of the resonator dimensions for realizing accurate measurements of speed of sound in another gas, for instance, argon.

2 Experimental Apparatus and Procedures

During 2003, we measured the acoustic and microwave resonance frequencies of a stainless-steel-walled spherical cavity filled with argon to perform primary acoustic gas thermometry in the temperature range from 234 to 380 K [4]. For the present work, we used the same resonator, materials, instrumentation, experimental procedures and methods, with a few exceptions that are listed and discussed below.

2.1 Preparation of a Misaligned Resonator for Simultaneous Acoustic and Microwave Measurements

In 2006, two additional holes were machined through the wall of the southern hemisphere of the resonator, bringing the total number of ports to four. Two ports were used for mounting 1/4" (0.64 cm) condenser microphones and the other two admitted antennae, thus allowing simultaneous measurement of acoustic and microwave resonances. The straight probe antennae used for the primary thermometry measurements were replaced with miniature copper loop probes to excite and detect both the TM and the TE classes of electromagnetic modes.

Then, we introduced the technique of deliberately displacing (*i.e.*, misaligning) one hemisphere relative to the other in their equatorial plane. This technique lifts the degeneracy of the microwave modes in a continuously variable, controllable manner, while maintaining the volume of the resonator constant. In preliminary tests, we discovered that the misalignment perturbed the average frequency of the microwave modes by approximately a quadratic function of the displacement and by an approximately linear function of frequency [8]. For the measurements reported here, the misalignment was as small as possible, consistent with lifting the degeneracy enough to fit the components of triply degenerate modes with a precision of 1 ppm or less. After this, desired misalignment was found by trial and error, the hemispheres were tightly bolted together, the angular orientation of the probes was adjusted, and the probes were withdrawn from the inner cavity volume to minimize coupling losses. The withdrawing of the probes drastically reduced the signal-to-noise (S/N) ratio and reduced from nine to five, the number of precisely-measurable, triply-degenerate modes that fell within the frequency range accessible to the network analyzer (13.5 GHz).

When the antennae were fixed in their final position, their coils protruded into the cavity by approximately 0.5 mm. To reduce the perturbations of the acoustic modes caused by the coils, we embedded them in an epoxy resin. The embedded antennae formed cone-shaped mounds that protruded into the cavity, as shown in Fig. 1. Since the mounds are acoustically "opaque" and electrically "transparent," they will introduce a difference between the volume of the cavity as sensed by the acoustic and the electromagnetic fields. To estimate this difference, we modeled the volume of the resin mounds as right circular cones with a base radius of 1.1 mm and a height of 0.5 mm. The ratio of the total volume of the two cones to the volume of the resonator is

Fig. 1 Loop probe used for microwave measurements: before (left) and after filling the housing duct with epoxy resin to avoid perturbations to the acoustic field

1.5 ppm, which is equivalent to 0.5 ppm of the radius of a geometrically perfect sphere of equal volume. This difference will be neglected during the present, preliminary measurements.

2.2 Dimensional Characterization of Some Geometrical Features of the Assembled Resonator

As an alternative, independent validation of the microwave determination of the resonator radius and its acoustic calibration with helium, which is described below, we investigated state-of-the-art mechanical measurements made with a coordinate measuring machine (CMM). A measurement plan is in progress, pursuing the following objectives: (i) definition of internal geometry of the two hemispherical halves composing the resonator; (ii) systematic measurement of the relative separation of microwave modes in different misalignment conditions (for these tests, CMM measurements on the outer surface of the assembled resonator are used to estimate the misalignment); and (iii) dimensional characterization of some geometrical details of the resonator, such as the height of a possible equatorial gap, and recession or protrusion of microphone and antennae housings.

In this work, a high accuracy CMM was used to characterize a few geometrical features of the assembled resonator. These include: (a) the relative position of the two hemispheres, and (b) the compression due to bolt tightening. For (a), the position of a hemisphere was measured relative to a coordinate system attached to the other hemisphere. Two steel balls were glued to the exterior of the equatorial collars, to mark their relative azimuthal phase (see Fig. 2). For each hemisphere, coordinates were measured on a circle on the exterior of the collar and the glued ball. The upper surface of the collar on the upper hemisphere was also measured. Then, a coordinate system was defined on the basis of features of the upper hemisphere: the xy plane was taken coincident with the top surface of the collar, the z axis through the collar center, and the x-axis through the projection of the ball center onto the xy plane. The position of the

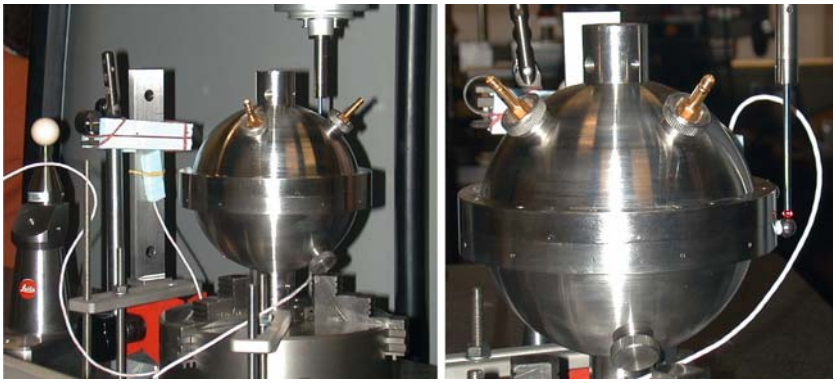

Fig. 2 Setup of CMM measurements on the assembled resonator

lower hemisphere was fully defined by the (x, y) coordinates of the center of its collar and by the azimuthal angle in the xy plane of the center of its ball. Finally, we computed the horizontal distance between the centers of the collars: $(46.7 \pm 0.2)\mu$m. This distance does not coincide with the misalignment of the two hemispheres, although we took it as the best estimate. The collars are external features, while the hemispheres are internal features: the two distances differ if the collars are not concentric with the hemispheres. Since the resonator was manufactured accurately, the concentricity errors are expected to be small, likely below 50 μm.

At the time of writing, measurements to determine the hemisphere compression caused by bolting are still underway; hereafter, we illustrate some details concerning the measurement procedure. The hemisphere compression is expected to occur mainly in the collars, where the bolts act. The deformation of the cavity near the interface between the hemispheres is expected to be much smaller. As a consequence, a direct—and simple—measurement of the collar thickness would have conveyed little information on the actual cavity deformation. Therefore, we chose to measure the distance between the cylindrical extensions (bosses) at the poles of each hemisphere (pole-to-pole distance), and monitor its variation caused by varying the bolting strength. Since the deformation is possibly sub-micrometric over a nominal size of 200 mm, special care was taken to account for thermal expansion. A compensation based on the resonator temperature only would not have been sufficient, because of the expansion affecting the CMM scales, which were not accessible to our temperature measurement. To overcome this, a calibrated gage block of the same nominal size as the pole-to-pole distance, was measured as well (Fig. 2), fixtured in the vertical position at the same height as the resonator. This way, any z axis error would have been the same for the resonator as for the gage block. The temperatures of the CMM scales were assumed stable during the few minutes required to measure the resonator and the gage block. All geometrical errors of the CMM, and the thermal expansion, could be compensated by the equation,

$$x_{20} = x\,\frac{l_{20}\,(1+\alpha_l\tau_l)}{l\,(1+\alpha_x\tau_x)} \approx x\,\frac{l_{20}}{l}\,(1+\alpha_l\tau_l-\alpha_x\tau_x)\,, \tag{1}$$

where x and l denote the CMM readings of the pole-to-pole distance and the gage block length, respectively, the subscript 20 indicates the reference temperature (20°C [9]), α_x and α_l are the thermal expansion coefficients, τ_x and τ_l are the deviations from the reference temperature, x_{20} is the measured, and l_{20} is the calibrated length of the gage block.

2.3 Thermometry

At the zeroth order, the speed of sound squared in a monoatomic gas is proportional to the thermodynamic temperature. Thus, near 273.16 K, a relative temperature uncertainty $u_r(T)$ of 2 ppm ($u(T) = 0.54$ mK) propagates into 1 ppm of v_{exp} . The temperature of the gas filling the resonator was inferred by the readings of two capsule-style 25.5Ω standard platinum resistance thermometers (CSPRTs) embedded in cylindrical extensions of the resonator poles. The resonator was enclosed within a pressure- and vacuum-tight stainless steel vessel that was immersed in a stirred liquid bath maintained near 273.16 K. During the time needed to record values for one acoustic isotherm (110 h), the average temperature of the resonator varied by as much as 1.5 mK, while the vertical gradient across the resonator, i.e., the difference between the temperature measured in the northern and southern resonator poles, varied between −0.05 and −0.3 mK. In 2006, one damaged CSPRT was replaced by a new one (HS 1421) having the same dimensions and filling gas mixture. This new thermometer was calibrated for the first time in July 2006 at the triple point of water (TPW) and at the melting point of gallium using the primary standard cells of INRIM. Several independent measurements of the CSPRT resistances at the TPW showed good repeatability, within 20μK. During the same period, one of the oldest CSPRTs (HS 124) was also checked at the TPW; it showed long-term stability (since 2001) of 0.1 mK. Self-heating effects were evaluated by repeatedly switching the current between 1 and 1.41 mA for both CSPRTs, while they were mounted inside the resonator's poles at a temperature near the TPW. During these tests, the resistances of the two CSPRTs increased slightly at a higher current by slight amounts (40 and 70$\mu\Omega$). The self-heating corrections were applied while estimating the average temperature of the gas T_{exp}. During January 2007, the linearity of the ASL F18 resistance bridge used for the present measurements was evaluated with a resistance bridge calibrator.

In summary, we estimate the uncertainty of the thermodynamic temperature measurements $U(T_{\mathrm{exp}}) = 0.21$ mK, after considering 6 factors: (1) the cell used to calibrate the CSPRTs took part in the recent CCT-K7 comparison, (2) the bridge non-linearity, (3) the bridge's reading uncertainty, (4) the CSPRTs' repeatability, (5) the values of T_{exp} in this work are within 0.015 K of the TPW, and (6) the uncertainty of the vertical temperature gradient across the resonator; the latter is the largest contribution to the overall temperature uncertainty.

2.4 Purity of Helium

Due to the high sensitivity of speed of sound in helium to impurities, the purity of the helium used in the experiment is of concern. Impurities have a two-fold effect on

our experimentally measured quantities: (i) impurities raise helium's refractive index and (ii) (with the exception of hydrogen) lower the speed of sound in helium. The supplier of helium specified its purity as 99.9999% by volume. We installed a nickel zeolite getter in the supply manifold. The manufacturer of the getter specified that it effectively removes common chemical reactants (CO, CO_2 O_2, H_2, H_2O) from noble gases at a sub-ppb level. Before their use, the resonator and the pressure vessel were carefully cleaned, repeatedly flushed with purified helium, and evacuated for at least 48 h. After this time, typical residual pressure readings were below 1×10^{-6} mbar in the evacuated part of the manifold. Despite these precautions, we had evidence that our sample was progressively contaminated by monitoring the acoustic resonance frequencies as a function of time. During a preliminary test at 100 kPa, we observed, for all the acoustic resonance frequencies, a secular change of −80 ppm/12 h. After baking the resonator under vacuum at 50°C for 48 h, this change was reduced by a factor of 25 at the same pressure, and it was below our detection capability at pressures over 300 kPa. Given the large effect of baking, we speculate that the contamination was mainly due to outgassing from the insulators in the microwave and/or microphone cables, the epoxy used to coat the antennae, or a virtual leak into the resonator. The remaining effects of outgassing, on the order of 0.3 ppm/h at 100 kPa, were tolerated for the present measurements. However, as discussed below, the progressive contamination of the sample might explain the disagreement between v_{exp} and v_{theory} at the lowest pressures.

2.5 Measurement Procedure

After the initial flushing, baking, and evacuation, gas was admitted into the pressure vessel and the resonator to raise the pressure to 800 kPa; the pressure was then lowered in 50 kPa steps to 100 kPa. The choice of these pressure limits was imposed by practical issues. The lowest pressure was determined by the low quality factor of acoustic resonances in helium (as compared to, for example, argon), the decreasing signal-to-noise ratio (S/N) of the acoustic signal, and the progressive contamination discussed above. The highest pressure was determined by our concern that the CSPRTs might rupture, or the pressure vessel bolts and electrical feedthroughs might fail. After each pressure step, 8 h were necessary for the resonator to equilibrate with the liquid bath. After this time elapsed, we recorded data for five triply degenerate microwave modes (TM11, TM12, TM13, TE11, and TE12), seven acoustic radial modes [(0,2) through (0,8)], temperature, and pressure. In-phase and quadrature amplitude data for acoustic and microwave resonances were, respectively, fitted to a single or the sum of three complex resonance functions plus a quadratic complex background [10]. The relative precision of the fitted microwave modes ranged from 0.3 ppm for mode TM12 to 1.7 ppm for mode TM13. The relative precision was inversely correlated to the mode amplitude, which depended on the efficiency of the coupling, and was practically independent of pressure. For the radial acoustic modes, the relative precision was proportional to the product $g(\mathrm{S/N})^{-1}$, where g is the half-width of the resonance. This product, a function of pressure and mode, ranges from a minimum of 4.6×10^{-8} for mode (0,4) at 800 kPa to a maximum of 2.6×10^{-6} for mode (0,8) at 100 kPa.

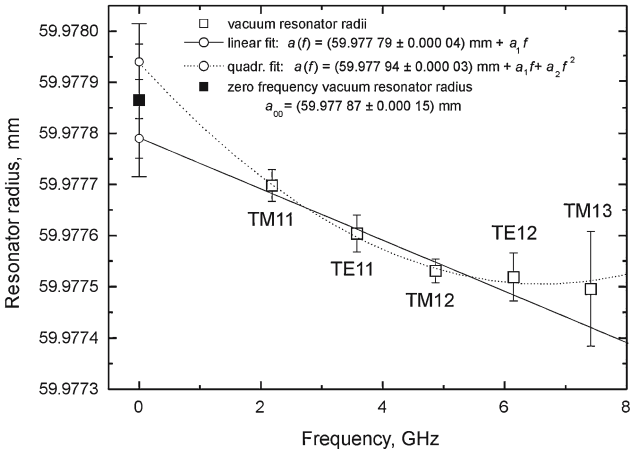

Fig. 3 Extrapolation to zero frequency of vacuum resonator radii obtained from five different microwave TM and TE modes near 273.16 K

3 Microwave Determination of the Resonator Radius

The average fitted experimental frequencies at each pressure $\langle f^{\mathrm{m}} \rangle_p$ for each microwave mode were corrected to account for the skin-effect perturbation by adding the average fitted experimental half-width $\langle f^{\mathrm{m}} + g^{\mathrm{m}} \rangle_p$. Alternatively, the half-widths may be calculated using published values of the resistivity of stainless steel [11]. If this alternative is taken, the quantities $\langle f^{\mathrm{m}} + g^{\mathrm{m}} \rangle_p$ increase by 3.5 ppm for modes TM12, TM13, TE11, and TE12, and by 6.0 ppm for mode TM11. The average ratio between the calculated and experimental half-widths is (0.95 ± 0.01) for all modes, and is inconsistent with the estimated 3% uncertainty associated with the literature value of resistivity for the same type of steel. This discrepancy is the largest uncertainty contribution to the present microwave determination of the resonator's radius.

The corrected frequencies were extrapolated with a quadratic function of the pressure to obtain corresponding vacuum frequencies $\langle f^{\mathrm{m}} + g^{\mathrm{m}} \rangle_0$ for each mode with a relative uncertainty from the fit, which varied from 0.1 ppm for mode TM12 to 0.8 ppm for mode TM13. From the results of the pressure fits, a value of the resonator radius at zero pressure for the n^{th} mode a_{0n} was calculated using the eigenvalues z_n^{m} of a geometrically perfect sphere and the speed of light in vacuum c_0 as: $a_{0n} = c_0 z_n^{\mathrm{m}} / \left(2\pi \langle f^{\mathrm{m}} + g^{\mathrm{m}} \rangle_0\right)$. The vacuum radii calculated from different modes and their frequency dispersion are shown in Fig. 3, where the displayed uncertainty of a_{0n} is dominated by the fitting precision of each microwave triplet.

We do not have a model that predicts the perturbations to the microwave frequencies induced by our deliberate misalignment of the resonator; thus, we rely on our observation (Fig. 3) that the dispersion of the radii is a monotonically decreasing function of the frequency. We extrapolated the radii from the different modes to a single, zero frequency vacuum radius, using both a weighted linear and a weighted quadratic function of the frequency. The results of these extrapolations are illustrated in Fig. 3. In contrast with our previous experience [8], the zero-frequency radii determined with these two

alternative functions are inconsistent, perhaps because we have fewer modes than in the previous work. Quite arbitrarily, we take their average as the best estimate for the vacuum resonator radius: $a_{00} = (59.97787 \pm 0.00015)$ mm, where the associated uncertainty (2.5 ppm) is equal to two times their difference. We note that perturbation theory has been extended to calculate second-order perturbations on radial and non-radial acoustic modes in resonators of arbitrary shape [12]. Therefore, we are optimistic that the corresponding problem for microwave modes will be solved soon and that, when our empirical extrapolation is replaced with theory, the 2.5 ppm extrapolation uncertainty will become much smaller.

The value of a_{00} was converted to the following function of temperature and pressure:

$$a_{00}(p, T) = a_{00}\left[1 + \alpha_{\text{th}}\left(T - \langle T_{\text{exp}}\rangle\right) - \frac{k_T}{3}p\right] \tag{2}$$

using the thermal expansion coefficient $\alpha_{\text{th}} = 1.58 \times 10^{-5}\,\text{K}^{-1}$ measured for the same resonator during previous thermometry experiments [4], and using the isothermal compressibility $k_T = 6.48 \times 10^{-12}\,\text{Pa}^{-1}$. This value of k_T was calculated from literature values of the adiabatic compressibility k_S [13], density ρ, and heat capacity C of 316 stainless steel using the thermodynamic relation: $k_T = k_S + \left[(3\alpha_{\text{th}})^2\, T/(\rho C)\right]$. In Eq. 2, $\langle T_{\text{exp}}\rangle = 273.1456\,\text{K}$ indicates the average temperature of the isotherm. In the present measurements, the temperature corrections to the radius were only a few parts in 10^8.

By direct measurements, we confirmed the procedure just described for calculating the isothermal compressibility k_T. To do so, we used the results of *ab initio* calculations of the properties of helium (molar polarizability, density virial coefficients, dielectric virial coefficients, diamagnetic susceptibility) [6] to calculate the refractive index of helium $n = \sqrt{\varepsilon_r \mu_r} = c_0/c$ (where ε_r is the relative dielectric permittivity, μ_r is the relative magnetic permeability, and c is the speed of light in helium as a function of temperature and pressure). The refractive index values were used to convert measured values of $\langle f^{\text{m}} + g^{\text{m}}\rangle_p$ to values of resonator radius using the relation $a(p, T)_n = cz_{\text{mn}}/\left(2\pi\langle f^{\text{m}} + g^{\text{m}}\rangle_p\right)$. When this was done, we obtained $k_{T\,exp} = (6.7 \pm 0.7) \times 10^{-12}\,\text{Pa}^{-1}$ as the measured isothermal compressibility of the *assembled resonator*. Remarkably, this value is consistent with the literature value reported above, and the values of radius obtained with this alternative procedure agree within 0.5 ppm with the prediction of Eq. 2 over the whole pressure range.

4 Acoustic Measurements in Helium

The fitted frequencies of the first seven radial acoustic modes in helium, (0,2) through (0,8), were corrected according to the classical model of acoustic propagation in a dissipative gas and the predictions of perturbation theory for a rigid acoustic spherical cavity [14]. We accounted for frequency shifts and/or energy losses induced by bulk effects, the presence of a thermal boundary layer (including the temperature-jump effect with the thermal accommodation coefficient $h = 1$, and the propagation

of a thermal wave into the shell), the coupling of gas and the breathing mode of shell motion, and the presence of a vent hole machined through the resonator wall. To calculate the corrections, the density of helium was obtained iteratively from the virial equation of state at fourth order, with values of the density virial coefficients from [7,15]. The thermal conductivity and viscosity of helium at zero-density were obtained from [7].

As an independent test of the validity of our acoustic model, we consider $\Delta g^a/f^a = \left(g^a_{\rm exp} - g^a_{cslc}\right) \Big/ f^a$, the differences between the experimental and calculated acoustic half-widths, scaled by the corresponding resonance frequencies f^a, as a function of the ratio between the radius of the resonator and the thermal penetration length (See Fig. 4). For the majority of modes, $10^6 \Delta g^a/f^a < 5$ holds over the whole pressure range and $10^6 \Delta g^a/f^a$ decreases at the lowest pressures. Figure 4 shows particularly large values of $10^6 \Delta g^a/f^a$ for mode (0,3) that increase from 15 to 70 ppm as the pressure increases. We speculate that this anomalous increase results from the proximity of the (0,3) mode (19.94–20.01 kHz) to the breathing mode of the shell, which was calculated to be 20.130 kHz. We remark that the contribution to the half-width predicted by the model by including the radiation losses from the shell outer surface [14] accounts for only about $1/7^{\rm th}$ of the experimental half-width. This observation leads to the conclusion that our current modeling of the shell effect is still unsatisfactory. We conjecture that the breathing mode of our shell differs significantly from that calculated, probably because the shell is non-uniform. The shell has an equatorial joint, and it is mechanically coupled to both the pressure vessel and to the container of the thermostatic bath. In order to improve our understanding of these effects, we plan to measure the breathing frequency and other possible resonances of the shell. Figure 4 shows that, to a lesser extent, similar arguments apply to modes (0,2) and (0,4). As observed and discussed in [4], the half-width of mode (0,2) appears to be influenced by the presence of the vent-hole in an unpredictable way. For these reasons, we decided to reject the data for modes (0,2), (0,3), and (0,4); they were not used for the final calculation of $v_{\rm exp}$. Finally, from examination of Fig. 4, it is apparent that mode (0,7) shows an increasing excess half-width at pressures below 200 kPa. This is probably due to an overlapping of mode (0,7) with its neighboring mode (13,2). However, this anomaly did not seem to affect the corrected frequency of mode (0,7), whose values were included in the final analysis.

The corrected acoustic frequencies were combined with the microwave estimate of the resonator radius to obtain experimental values of the speed of sound in helium $v_{\rm exp}$. We calculated theoretical values of the speed of sound $v_{\rm theory}$ as a function of pressure using the virial expansion, with values for the second acoustic virial coefficient from the *ab initio* results in [7] and values of the third virial coefficient, and their temperature derivatives from recent $p\rho T$ measurements [15]. The three different frames in Fig. 5 show the fractional differences $\Delta v = \left(v_{\rm exp} - v_{\rm theory}\right) \Big/ v_{\rm theory}$ in ppm, as a succession of acoustic perturbations are taken into account. When applying only the boundary layer correction (Fig. 5a), the deviations of modes (0,3) and (0,2) show the typical linear dependence on pressure caused by the shell's admittance. The sign of the pressure slope for the (0,2) mode is negative and that of the (0,3) mode is positive. This indicates that the breathing frequency of the shell $f_{\rm breath}$ falls in the range

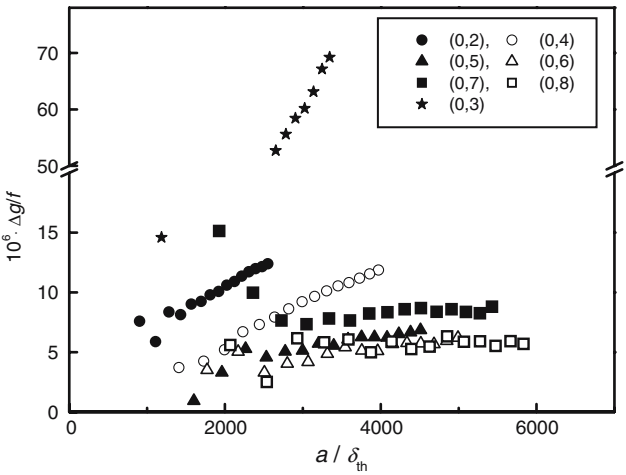

Fig. 4 Excess half-widths for seven acoustic purely radial modes scaled by $10^6/f$ as a function of the ratio between the nominal resonator radius and the thermal penetration length

$f_{0,2} < f_{\text{breath}} < f_{0,3}$. This contradicts the prediction that $f_{03} < f_{\text{breath}}$. Remarkably, the dispersion of all other modes (with the possible exception of mode (0,8) at the lowest pressures) is within 5 ppm. By applying the shell correction using the predicted value of f_{breath} (Fig. 5b), the deviations of mode (0,3) increase by a factor of 50. On a different scale, the results for mode (0,2) are in better agreement with those of other modes, while mode (0,4) gets to be an outlier, shifting away from the group by 6 ppm.

Finally, the effect of the correction due to the presence of the gas-inlet hole, which was modeled as a uniform duct, 4 mm long and 1 mm wide, is shown in Fig. 5c. The inlet hole correction is largest for the (0,2) mode (10 ppm) and it is close to zero for mode (0,7). As a result, the dispersion among the modes is further increased. As previously noticed and discussed in [4,5], the perturbative model that accounts for the effects of openings in the resonator wall does not make accurate predictions for this resonator. We hope to solve this problem by closing the vent-hole with a small, electrically-actuated valve that mates with the inner surface of the resonator in its closed position.

In the above analysis, the effect of geometrical perturbations has not been considered. To the best of our knowledge, the deliberately imposed misalignment of the two hemispheres is the largest geometric perturbation. We will analyze the effects of geometrical perturbations on the acoustic eigenfrequencies after we obtain a complete set of CMM measurements that might reveal, for example, differences in the shape or the average diameters of the two hemispheres.

5 Comparison of Acoustic and Microwave Radii

To test the consistency of our microwave and acoustic results and to assess the uncertainty of our current measurements, we calculated the differences $v_{\text{exp}} - v_{\text{theory}}$, and displayed them as a fraction in Fig. 6. We used the acoustic data from the modes (0,5),

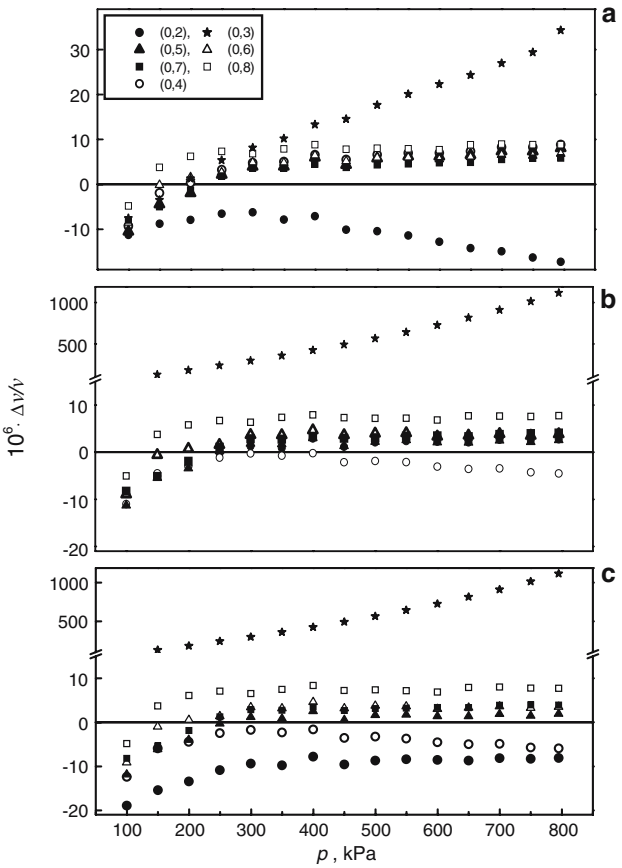

Fig. 5 Relative differences $(v_{\mathrm{exp}} - v_{\mathrm{theory}})/v_{\mathrm{exp}}$ expressed in ppm for seven radial acoustic modes. The three panels display the effect of accounting for different perturbations: (**a**) boundary layer correction only; (**b**) boundary layer + shell admittance; and (**c**) boundary layer + shell admittance + vent-hole admittance

(0,6), (0,7), and (0,8), because of their comparatively small excess half-widths. The acoustic data were averaged and combined with our determination of the resonator radius.

The error bars in Fig. 6 display the overall uncertainty of v_{exp}, which we estimated as the sum in quadrature of the contributions from three sources: (a) the uncertainty of the resonator radius (as discussed in Sect. 3, this is a conservative estimate, which encompasses the results of the extrapolations of microwave data to zero frequency with two different empirical functions); (b) the uncertainty of the corrected acoustic frequencies, which has a minor contribution that accounts for the imprecision of raw acoustic data, and a major contribution from the discrepancies among the results of the selected modes after applying corrections for known perturbations; and (c) the uncertainties from INRIM standards of temperature and pressure, and our laboratory realization of these quantities. As discussed in Sect. 2.3, $u(T_{\mathrm{exp}}) = 0.21\,\mathrm{mK}$, which is negligible in the present context; however, $u(p_{\mathrm{exp}})$ ranges from 60 Pa at 100 kPa to

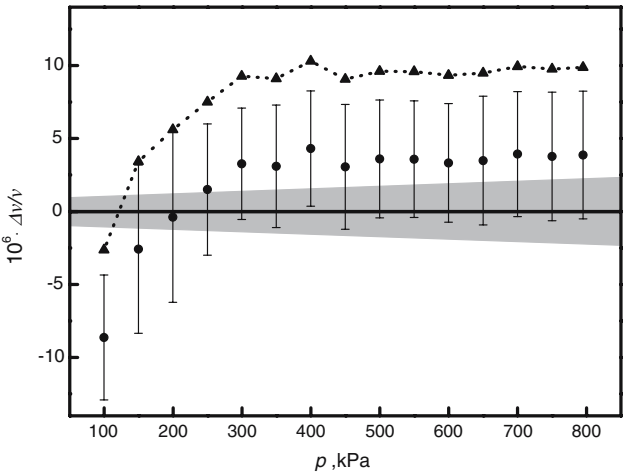

Fig. 6 Comparison between v_{exp} and v_{theory} for averaged acoustic data. Full circles and error bars apply to a microwave radius determined using frequencies corrected by experimental half-widths; full triangles apply to a frequency correction using literature resistivity values. The shaded area displays the uncertainty of v_{theory}

300 Pa at 800 kPa, and these values propagate into $u_r(v_{\mathrm{exp}}) = 0.3$ and 1.5 ppm, respectively. Altogether, the relative uncertainty of v_{exp} varies between 3.8 and 5.8 ppm. In Fig. 6, the open circles connected by a dotted line display the effect of using calculated, instead of measured half-widths for the skin-effect correction of microwave frequencies. The resulting microwave radius is larger by 6.0 ppm, (59.97823 ± 0.00036) mm.

The shadowed area in Fig. 6 displays the relative uncertainty of v_{theory}, with contributions from the uncertainty of the second virial coefficient $B(T)$ and its temperature derivatives [7], and the uncertainty of the third virial coefficient of helium $C(T)$, from recent experimental results [15]. These sources contribute to an overall uncertainty $u_r(v_{\mathrm{theory}})$, which ranges from 1.2 ppm at 100 kPa to 3.4 ppm at 800 kPa.

Figure 6 shows that v_{exp} and v_{theory}, or equivalently the *microwave* and the *acoustic* radii, sensed by the microwave and acoustic field excited within the resonator, do agree within their combined uncertainties between 150 and 800 kPa. We attribute the negative larger deviations below 250 kPa to the progressive contamination of our helium sample. While we have no information concerning the nature and the concentration of the contaminants, we observe that the relative difference of -9 ppm between v_{exp} and v_{theory} at 100 kPa would be, for example, explained by the presence of argon in helium with a relative molar concentration of 2 ppm.

6 Conclusions and Anticipated Improvements

In order to determine R and k with an uncertainty of 1 ppm or less using the apparatus, methods, and procedures described in this work, major problems mentioned above must be solved. Although misalignment is a simple geometrical perturbation that greatly increases the precision of the microwave frequency determination, its

influence on both the acoustic and microwave eigenfrequencies needs further theoretical modeling and/or experimental verification. When the program of CMM measurements described above is completed, we will have data to support this verification.

The uncertainty of the microwave determination of the radius of our stainless steel resonator would be significantly reduced if we had an independent value of its electrical resistivity. Alternatively, the resonator might be fabricated or plated with a metal such as copper that has a much lower resistivity.

The current mode-dependent discrepancies of our acoustic data might be reduced by a measurement of the shell's resonance frequencies and by valving off the gas inlet hole during the acoustic measurements.

Our limited ability to maintain the purity of a helium sample prevented us from determining a reliable estimate of the speed of sound at zero pressure by extrapolation of the experimental data. If the source of the contamination cannot be eliminated, its effect might be minimized by adopting a flowing gas technique [5].

Acknowledgments We are indebted to Davide Corona of the Mechanics Division of INRIM, who assisted during the CMM measurements. We thank Mike Moldover for his useful comments and careful reading of the manuscript.

References

1. M.R. Moldover, S.J. Boyes, C.W. Meyer, A.R.H. Goodwin, J. Res. Natl. Inst. Stand. Technol. **104**, 11 (1999)
2. G.F. Strouse, D.R. Defibaugh, M.R. Moldover, D.C. Ripple, in *Temperature: Its Measurement and Control in Science and Industry*, vol. 7, Part 1, ed. by D.C. Ripple (AIP, New York, 2003), pp. 31–36
3. M.B. Ewing, J.P.M. Trusler, J. Chem. Thermodyn. **32**, 1229 (2000)
4. G. Benedetto, R.M. Gavioso, R. Spagnolo, P. Marcarino, A. Merlone, Metrologia **41**, 74 (2004)
5. L. Pitre, M.R. Moldover, W.L. Tew, Metrologia **43**, 142 (2006)
6. R.M. Gavioso, E.F. May, M.R. Moldover, J.W. Schmidt, Y. Wang, in *Conf. Digest of 2006 Conference on Precision Electromagnetic Measurements*, ed. by F. Levi, M. Pisani (CLUT, Torino, 2006), pp. 30–31
7. J.J. Hurly, J.B. Mehl, J. Res. Natl. Inst. Stand. Technol. **112**, 75 (2007)
8. R.M. Gavioso, G. Benedetto, P.A. Giuliano Albo, A. Merlone, A. Balsamo, R. Spagnolo, in *Talks of the 221st PTB Seminar Workshop on Progress in Determining the Boltzmann Constant*, ed. by B. Fellmuth, J. Fischer (Report PTB-Th-3, Braunschweig, in press)
9. ISO 1:2002–Geometrical Product Specifications (GPS)–Standard reference temperature for geometrical product specification and verification (2002)
10. E.F. May, L. Pitre, J.B. Mehl, M.R. Moldover, J.W. Schmidt, Rev. Sci. Instrum. **75**, 3307 (2004)
11. A.F. Clarke, G.E. Childs, G.H. Wallace, in *Adv. Cryo. Eng.*, vol. 15, ed. by K.D. Timmerhaus (Plenum, New York, London, 1970), pp. 85–90
12. J.B. Mehl, J. Res. Natl. Inst. Stand. Technol. **112**, 163 (2007)
13. H.M. Ledbetter, J. Appl. Phys. **52**, 1587 (1981)
14. M.R. Moldover, J.B. Mehl, M. Greenspan, J. Acoust. Soc. Am. **79**, 253 (1986)
15. M.O. McLinden, C. Lösch-Will, J. Chem. Thermodyn. **39**, 507 (2007)